Physics Letters B 838 (2023) 137685

Contents lists available at ScienceDirect

Physics Letters B

journal homepage: www.elsevier.com/locate/physletb

Elliptic flow in heavy-ion collisions at intermediate energy: The role of impact parameter, mean field potential, and collision term

Bo Gao [a,b], Yongjia Wang [a,*], Zepeng Gao [c,a], Qingfeng Li [a,d,**]

[a] School of Science, Huzhou University, Huzhou 313000, China
[b] School of Physical and Electronic Engineering, Shanxi University, Taiyuan 030006, China
[c] Sino-French Institute of Nuclear Engineering and Technology, Sun Yat-sen University, Zhuhai 519082, China
[d] Institute of Modern Physics, Chinese Academy of Science, Lanzhou 730000, China

ARTICLE INFO

Article history:
Received 15 October 2022
Received in revised form 16 December 2022
Accepted 7 January 2023
Available online 11 January 2023
Editor: B. Balantekin

ABSTRACT

Within the ultrarelativistic quantum molecular dynamics (UrQMD) model, by reversely tracing nucleons that are finally emitted at mid-rapidity ($|y_0| < 0.1$) in the entire reaction process, the time evolution of elliptic flow (v_2) of these traced nucleons is studied in Au+Au collisions at beam energy of 0.4 GeV/nucleon with different impact parameters. The initial value of v_2 is positive and increases with impact parameter, it then decreases as time passes and tends to saturate at a negative value. It is found that nucleon-nucleon collisions always suppress the value of v_2 (enhance the out-of-plane emission), while the nuclear mean field potential effect is more complex, which depends on both impact parameter and reaction time. The most relevant density probed by v_2 of nucleons at mid-rapidity is found to be $\sim$ 60% of the maximum density reached during the collisions.

© 2023 Huzhou University. Published by Elsevier B.V. This is an open access article under the CC BY license (http://creativecommons.org/licenses/by/4.0/). Funded by SCOAP[3].

1. Introduction

Collective flow which characterizes the collective motion of the produced particles in heavy-ion collisions (HICs) is of great importance for studying the underlying physics [1–9]. It provides indirect access to the properties of the hot and dense matter created in HICs, and therefore has been extensively studied both theoretically and experimentally over a broad energy range. At intermediate energies (with beam energy of several hundreds MeV per nucleon), experimental data of collective flow are often compared with theoretical calculations performed with transport models in order to infer physical information. These include the nuclear equation of state (EOS), the in-medium nucleon-nucleon (NN) cross section, the nucleon effective mass, and the nuclear symmetry energy; see e.g., Refs. [10–22].

The directed flow (v_1, also called in-plane flow) and the elliptic flow (v_2, also called out-of-plane flow) are two lower-order components widely studied in HIC at intermediate energies [1,12,16]. The former characterizes the particle collective motion in the reaction plane (the plane spanned by the impact parameter vector x and the beam direction z). The latter describes the particle collective motion in the direction perpendicular to the reaction plane. Elliptic flow is one of the most important observables in HICs not only at intermediate energies but also at relativistic energies. Elliptic flow at intermediate energies has attracted considerable attention because it exhibits good sensitivity to the not well constrained nuclear equation of state [3,23–26]. It is found experimentally that v_2 depends on beam energy, impact parameter, particle species, and colliding nuclei [12,27,28]. From theoretical point of view, v_2 is highly sensitive to the nuclear mean field potential and nucleon-nucleon (NN) collisions [29–35]. However, a quantitative attribution of these effects to v_2 is still unclear.

In the present work, within the ultrarelativistic quantum molecular dynamics (UrQMD) model, the evolution of v_2 of free nucleons at mid-rapidity in the final state is traced over the entire reaction history. The contributions of each issue to v_2 are disentangled by recording the change of momenta. The paper is organized as follows. In Sec. 2, the method to calculate the individual contributions from the nuclear mean field potential and NN collisions to v_2 is presented. Results and discussions are presented in Sec. 3. A summary is given in Sec. 4.

2. Methodology

The elliptic flow parameter v_2 is the second-order coefficient in the Fourier expansion of the azimuthal distribution of emit-

* Corresponding author.
** Corresponding author at: School of Science, Huzhou University, Huzhou 313000, China.
E-mail addresses: wangyongjia@zjhu.edu.cn (Y. Wang), liqf@zjhu.edu.cn (Q. Li).

https://doi.org/10.1016/j.physletb.2023.137685
0370-2693/© 2023 Huzhou University. Published by Elsevier B.V. This is an open access article under the CC BY license (http://creativecommons.org/licenses/by/4.0/). Funded by SCOAP[3].

ted particles, $v_2 = \langle V_2 \rangle = \left\langle \frac{p_x^2 - p_y^2}{p_t^2} \right\rangle$. Here, p_x and p_y are the two components of the transverse momentum, $p_t = \sqrt{p_x^2 + p_y^2}$, and the angular bracket denotes an average over all considered particles of all events. (Throughout this letter, uppercase V_2 represents $\frac{p_x^2 - p_y^2}{p_t^2}$ of a nucleon). For a certain particle species, v_2 depends both on the rapidity y_z and the transverse momentum p_t. Usually, the scaled unit $y_0 \equiv y_z/y_{1\mathrm{cm}}$ (the subscript 1cm denotes the incident projectile in the center-of-mass system) is used instead of y_z [12]. In HICs with mass-symmetric projectile-target combination, the v_2 is an even function of y_0. v_2 of nucleons at mid-rapidity ($y_0 \sim 0$) is of great importance because these nucleons are expected to emerge from the most compressed region, carrying information of the hot and dense matter that is formed in HICs. We therefore focus on the v_2 of free nucleons at mid-rapidity ($|y_0| < 0.1$) in this study.

To study HICs at intermediate energies, the following density- and momentum-dependent potential is frequently used in QMD-like models [34–37],

$$U = \alpha \cdot (\frac{\rho}{\rho_0}) + \beta \cdot (\frac{\rho}{\rho_0})^{\gamma} + t_{\mathrm{md}} \ln^2[1 + a_{\mathrm{md}}(\mathbf{p}_i - \mathbf{p}_j)^2]\frac{\rho}{\rho_0}. \quad (1)$$

In this work, $\alpha = -398$ MeV, $\beta = 334$ MeV, $\gamma = 1.14$, $t_{\mathrm{md}} = 1.57$ MeV, and $a_{\mathrm{md}} = 500\ c^2/\mathrm{GeV}^2$ are adopted in UrQMD model, which yields a soft and momentum-dependent EOS with the incompressibility $K_0 = 200$ MeV. The symmetry potential derived from the SV-sym34 interaction is chosen which yields the nuclear symmetry energy with slope parameter of 81.2 MeV. The FU3FP4 parametrization [32] for the in-medium NN cross section and an isospin-dependent minimum spanning tree (isoMST) method [38] for cluster recognition are used. It is found, with appropriate choices of the above parameters, that the recent published experimental data at intermediate energies can be reproduced fairly well with the UrQMD model [17,18,35].

In the framework of the UrQMD model [39,40], the momentum of each nucleon can be changed either by the force caused by the nuclear mean field potential or by nucleon-nucleon (NN) scattering. As a many-body microscopic transport model, UrQMD allows recording of momentum changes of each nucleon in the mean field propagation and NN scatterings. The variation of v_2 caused by a collision can be calculated as

$$\Delta v_2^{\mathrm{coll}}(t) = \left\langle V_2^{\mathrm{aft.coll}}(t) - V_2^{\mathrm{bef.coll}}(t) \right\rangle. \quad (2)$$

The average is taken over all the traced nucleons within the time step Δt which is set to 1 fm/c in this work. The variation of v_2 due to the mean field potential can be calculated using the momenta of nucleons after and before mean field propagation,

$$\Delta v_2^{\mathrm{mf}}(t) = \left\langle V_2^{\mathrm{aft.mf}}(t + \Delta t) - V_2^{\mathrm{bef.mf}}(t) \right\rangle. \quad (3)$$

Together, the variation of v_2 can be obtained as follows

$$\Delta v_2(t) = \Delta v_2^{\mathrm{mf}}(t) + \Delta v_2^{\mathrm{coll}}(t). \quad (4)$$

3. Results and discussions

It is our goal to quantify the effects of initial geometry, mean field potential, and collision term to v_2 in HICs at intermediate energies. Note that in Ref. [30] the contributions of the nuclear mean field potential and NN collisions to v_2 in HICs at intermediate energies with a fixed impact parameter $b = 6$ fm were analyzed, and found that v_2 is more affected by potential effects. It is well known that v_2 depends heavily on impact parameter, thus a detailed study of the origin of the elliptic flow and its dependence on the impact parameter is needed to accurately characterize these contributions.

In the present work, Au+Au collisions at E_{lab} = 0.4 GeV/nucleon with impact parameters $b = 2$, 4, 6, 8, and 10 fm are simulated. Momenta of free protons and neutrons finally emitted at mid-rapidity ($|y_0| < 0.1$) are traced during the entire evolution of the collision and the v_2 development is investigated. The average number of traced free nucleons are 27.5, 21.2, 14.7, 8.9, and 4.2 for $b = 2$, 4, 6, 8, and 10 fm, respectively. More than 50 000 events for each impact parameter are calculated such that the statistical errors are negligible on the scale of the plots.

Fig. 1 displays the locations and momentum directions of the traced nucleons in the reaction plane at $t = 0$, 10, 16, 20, 30, 40 fm/c. One sees that p_x of the most traced nucleons are along the direction to the coordinate origin, because these nucleons have higher probability to experience a collision. Collisions are the main reason making the initial nucleons (with large $|p_z|$ and $y_0 \approx \pm 1$) emerge in the mid-rapidity (with almost zero p_z and $y_0 \approx 0$) region at the final state. In addition, it can be seen that although most of the traced nucleons are located in the central region where density is higher than the normal density, there are still a few of the traced nucleons located away from the central region; see e.g., Fig. 1(c). This implies that densities probed by v_2 of nucleons at mid-rapidity should be smaller than densities in the central region.

Fig. 2 shows the time evolution of v_2 of the traced nucleons emerging at mid-rapidity in the final state. At the initial time, v_2(t=0 fm/c) is non-zero, indicating that those nucleons are not randomly "selected" out of the uniform distribution in the initial state. This is especially so for large b where v_2(t=0 fm/c) is positive because nucleons with larger $|p_x|$ and smaller $|p_y|$ tend to have higher probability to experience NN scattering and finally emerge at midrapidity. This effect becomes more important with increasing impact parameter. v_2 decreases as time passes and approaches to zero at about $t = 10$ fm/c. This is mainly caused by the nuclear mean field potential, as collisions are rare before this time, which will be more clearly seen in Fig. 3. v_2 further decreases to negative value and tends to saturate as the reaction proceeds. In the case of $b = 10$ fm, the magnitude of v_2 first decreases to a minimum value at about $t = 25$ fm/c and then it slightly increases to the saturation value. It is mainly caused by the attraction from target- and projectile-like fragments in very peripheral collisions. At the final state, v_2 is negative because of the blocking by spectators–nucleons emitted in the reaction plane direction encounter spectators and are redirected, leading to the squeeze-out pattern. We note that in Refs. [24,41–48], the time evolution of v_2 was analyzed for particles emitted in the vicinity of a given time or up to a particular time, different from the present study.

The contributions of the mean field potential $\Delta v_2^{\mathrm{mf}}(t)$ and NN collisions $\Delta v_2^{\mathrm{coll}}(t)$ to v_2 of the traced nucleons are illustrated in Fig. 3. Note that v_2 in Au+Au collisions with impact parameter $b = 2$ fm is too small to get distinct values of $\Delta v_2^{\mathrm{mf}}(t)$ and $\Delta v_2^{\mathrm{coll}}(t)$, thus the result for $b = 2$ fm is not presented in the figure. At the initial time, $\Delta v_2^{\mathrm{coll}}(t)$ is zero because it takes approximately 5 fm/c for target and projectile nucleons to encounter each other. The value of $\Delta v_2^{\mathrm{coll}}(t)$ is always negative which indicates NN collision enhances the signal of out-of-plane elliptic flow (decreases the value of v_2). This is due to the effects of Pauli blocking by the spectator nucleons, because the outgoing nucleons along the reaction plane will be blocked. The value of $\Delta v_2^{\mathrm{mf}}(t)$ can be either negative or positive, depending on the impact parameter and time. At the initial time, $\Delta v_2^{\mathrm{mf}}(t)$ is positive (negative) for small (large) b because of the negative (positive) v_2, which can be understood from the fact that the mean field potential tends to attract nucleons until the target and projectile encounter with each other. As the collision process gives rise to a region of high density, the mean field potential becomes repulsive and tends to enhance the

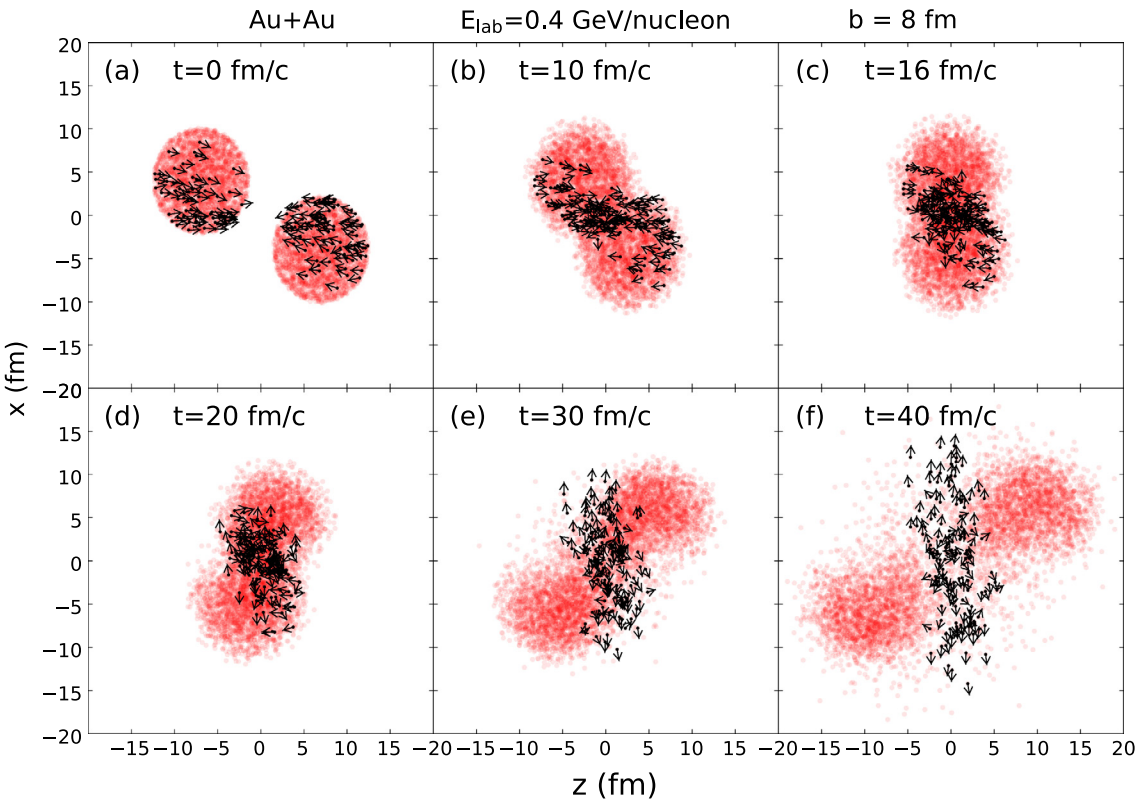

Fig. 1. Particle scatter plot in the reaction plane for Au + Au collisions with impact parameter $b = 8$ fm and beam energy $E_{\rm lab} = 0.4$ GeV/nucleon. Solid dots with arrows represent the traced nucleons, while circles denote other nucleons. The arrows denote the direction of the momentum vector (p_x, p_z). Results from 15 random events are displayed.

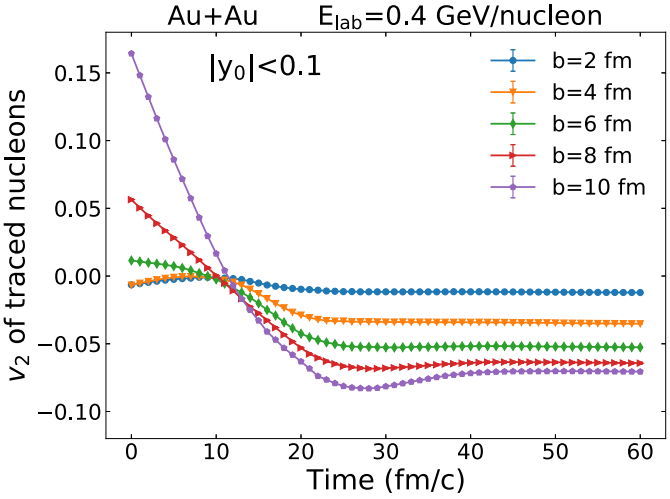

Fig. 2. Time evolution of v_2 of the traced nucleons finally emitted at mid-rapidity ($|y_0| < 0.1$) with different impact parameters.

out-of-plane emission (decrease the value of v_2), hence one sees negative $\Delta v_2^{\rm mf}(t)$. In large impact parameter cases of $b = 8$ and 10 fm, $\Delta v_2^{\rm mf}(t)$ can become positive during the expansion stage because of the attraction from target- and projectile-like fragments. The saturation time $t_{\rm sat}$, which is defined when the absolute value of $\Delta v_2(t)/dt$ is smaller than 0.0001 c/fm, increases from 26 fm/c to 45 fm/c when the impact parameter increases from 4 fm to 10 fm. This late saturation time is caused by the presence of spectators in peripheral collisions.

If one compares $\Delta v_2^{\rm mf}(t)$ with $\Delta v_2^{\rm coll}(t)$, it is found that, the mean field potential plays a dominant role in v_2 evolution until $t \approx 8$ fm/c for $b = 4$ fm and $\approx$20 fm/c for $b = 10$ fm. Then the collision effects become dominant and their contributions gradually weaken and eventually disappear as NN scatterings cease. For very peripheral collisions, the mean field potential may dominate the evolution of v_2 again at later times due to the attraction caused by target- and projectile-like fragments.

The time evolution of NN collision rate is important to understand their effect in the evolution of v_2. The number of collisions per event and the number of collisions per nucleon experienced by the traced nucleons are plotted as a function of time in Fig. 4 (a) and (b), respectively. It can be seen that, when b is varied from 2 fm to 10 fm, the average collision number per event decreases dramatically, while the average collision number per traced nucleon decreases only weakly. It is the reason why $\Delta v_2^{\rm coll}(t)$ in Fig. 3 changes weakly (compared to $\Delta v_2^{\rm mf}(t)$) with impact parameter. During the whole reaction, the average number of collisions experienced by the traced nucleons ($n_{\rm coll}$) varies from 2.8 to 2.0 when b increases from 2 to 10 fm. The inverse of $n_{\rm coll}$ is proportional to the Knudsen number (Kn), which can be used to quantify the degree of perfection of fluid [49,50]. Ideal hydrodynamics is the limit Kn $\to$ 0, that corresponds to infinite scattering rates, this is the perfect-fluid limit. Whereas the limit Kn $\to +\infty$ corresponds to free streaming particles. The Knudsen number has been discussed in the studies of ultrarelativistic heavy ion collisions, e.g., at RHIC and LHC energies, where hydrodynamical models are usually applied. In the present studied energy, the system is away from the hydrodynamic limit, although the obtained Kn is similar to that estimated at the center-of-mass energy $\sqrt{s_{NN}} = 200$ GeV [49,51]. Note that $n_{\rm coll}$ has a different meaning in our work and in Refs. [49,51]. $n_{\rm coll}$ studied in the present work corresponds to the typical number of collisions that an initial nucleon experienced in order to emerge in the mid-rapidity at the final state. While the inverse Knudsen number discussed at RHIC and LHC energies denotes the average collision number experienced by a particle

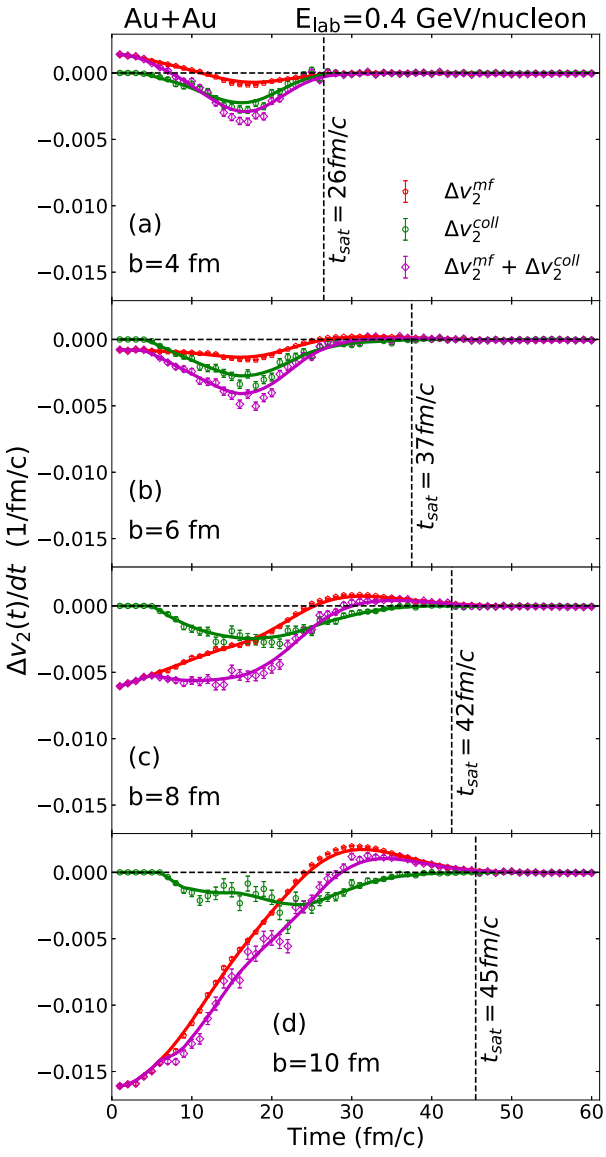

Fig. 3. The time evolution of $\Delta v_2^{\rm mf}(t)$, $\Delta v_2^{\rm coll}(t)$, and their sum Δv_2. Lines are smooth curves drawn through the calculated points. The saturated time $t_{\rm sat}$ for each impact parameter is indicated by italic text along the vertical dashed line.

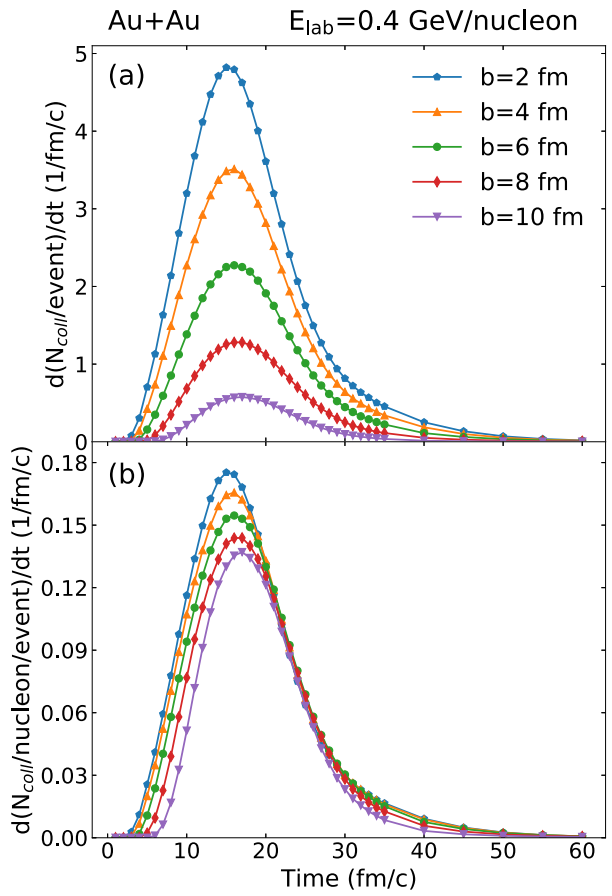

Fig. 4. Upper panel: The time evolution of the number of collisions per event experienced by the traced nucleons. Lower panel: The same as the upper panel but for the number of collisions per event per nucleon.

before freezing out. Further studies of Knudsen number and its relation to v_2 in HICs from intermediate to relativistic energies are certainly required to get a whole physical picture. In addition, it is found that there are still a few collisions even after $t_{\rm sat}$, especially for less peripheral collisions, i.e., $b = 4$ fm. These particles emerging from late collisions are less blocked by the spectator nucleons (i.e., isotropic scattering is dominant), and their contributions to v_2 are negligible.

The role of the surrounding nucleons in the evolution of elliptic flow is also very important, although we focus on the nucleons that emitted at mid-rapidity throughout the paper. At the present studied energy, the surrounding nucleons block the escape of nucleons along trajectories in the reaction plane and squeeze nucleons out the compressed region in directions perpendicular to the reaction plane. These two effects are naturally comprised in the mean-field propagation and nucleon-nucleon scattering of transport model.

It is known that HICs are non-equilibrium and dynamical processes, and the density of the created environment changes with reaction time. It is therefore of interest to know which densities are probed by or mostly related to v_2 of nucleons at mid-rapidity. This is an important question especially for investigating the density-dependent nuclear symmetry energy with elliptic flow ratio. To that end, the average density at the central region (ρ_c) of Au+Au collisions and the density experienced by the traced nucleons (ρ_t) are plotted in Fig. 5. At the initial time, ρ_c is smaller than ρ_t because there are no nucleons located at the coordinate origin at $t = 0$ fm/c. Further, it can be seen that not only the peak value of ρ_t is smaller than that of ρ_c, but also the duration of high density conditions in ρ_t is shorter than that in ρ_c. In addition, one finds that the standard deviation of ρ_t is much larger than that of ρ_c, because the traced nucleons may come from a variety of spatial regions with different densities, which can be easily understood from Fig. 1. To quantify densities that are mostly related to v_2 of nucleons at mid-rapidity, the Δv_2 weighted average density is calculated as follows,

$$\langle\rho\rangle_{v_2} = \frac{\int_0^{t_{sat}} |\Delta v_2(t)|\rho_t(t)dt}{\int_0^{t_{sat}} |\Delta v_2(t)|dt}. \quad (5)$$

The obtained $\langle\rho\rangle_{v_2}$ are 0.206 and 0.145 fm^{-3} ($1.3\rho_0$ and $0.9\rho_0$) for $b = 4$ and 10 fm, respectively. These values are close to that obtained in Ref. [29], where the force (due to the nuclear mean field potential) weighted density is obtained to be 0.187 ± 0.07 fm^{-3} for the same system and beam energy but with $b = 3$ fm and $|y_0| < 0.8$. Moreover, in Ref. [14], by thoroughly analyzing the elliptic flow difference resulting from switching the density-dependent nuclear symmetry energy at certain density regions, the maximum sensitivity of the neutron-proton elliptic flow ra-

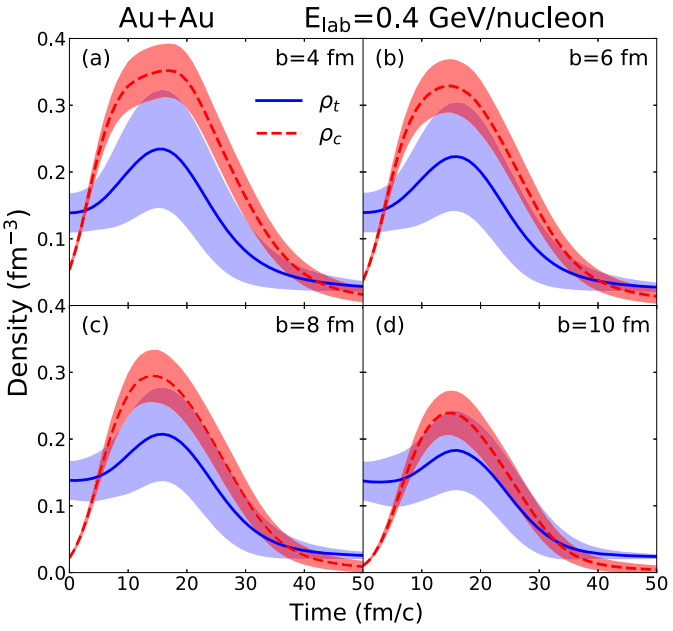

Fig. 5. The time evolution of the average density at the central region (ρ_c, dashed line) and density experienced by the traced nucleons (ρ_t, solid line). The curves and shaded bands denote the mean and the standard deviation, respectively.

tio lies in the $(1.4\sim1.5)\rho_0$ region, this value is close to our result even though a different method and transport model are applied. In Ref. [52], the densities weighted by the pion production rate and the force acting on Δ resonance are obtained to be 0.272 and 0.224 fm^{-3} ($1.7\rho_0$ and $1.4\rho_0$) for the same system and beam energy but for more central collisions, respectively. Taken together, these calculations indicate that the most relevant density probed by v_2 of nucleons at mid-rapidity in Au+Au collisions at $E_{\rm lab} = 0.4$ GeV/nucleon is around $(0.9\sim1.3)\rho_0$ (dependent of the impact parameter), and is only about 60% of the maximum density created during the reaction and is smaller than that probed by the pion observable.

4. Summary

To summarize, by reversely tracing nucleons finally emitted at mid-rapidity ($|y_0| < 0.1$) in the entire reaction process, the contributions of the nuclear mean field potential and NN collisions to the elliptic flow evolution in Au+Au collisions at beam energy of 0.4 GeV/nucleon with different impact parameters are studied. At the initial time, v_2 of the traced nucleons are positive and increase with increasing b, because the initial nucleons with positive v_2 have high probability appeared at mid-rapidity. The value of v_2 decreases as time passes and approaches zero at about $t = 10$ fm/c, mainly caused by the nuclear mean field potential. As the reaction proceeds, the contributions of the NN collisions to v_2 become more important, and v_2 further decreases to negative values and then tends to saturate. It is found that NN collisions always suppress the value of v_2, while the mean field potential may slightly raise the value of v_2 during the expansion stage in peripheral reactions. The most relevant density probed by v_2 of nucleons at mid-rapidity lies in $(0.9\sim1.3)\rho_0$ and dependent of the impact parameter. Their values are found to be $\sim$ 60% of the maximum density reached during the collisions.

Declaration of competing interest

The authors declare that they have no known competing financial interests or personal relationships that could have appeared to influence the work reported in this paper.

Data availability

Data will be made available on request.

Acknowledgements

We thank Wolfgang Trautmann for a careful reading of the manuscript and valuable communications. We acknowledge fruitful discussions with Yingxun Zhang and the TMEP group. The authors are grateful to the C3S2 computing center in Huzhou University for calculation support. The work is supported in part by the National Natural Science Foundation of China (Nos. U2032145, 11875125, and 12147219), the National Key Research and Development Program of China under Grant No. 2020YFE0202002.

References

[1] W. Reisdorf, H. Ritter, Collective flow in heavy-ion collisions, Annu. Rev. Nucl. Part. Sci. 47 (1) (1997) 663–709.
[2] N. Herrmann, J.P. Wessels, T. Wienold, Collective flow in heavy-ion collisions, Annu. Rev. Nucl. Part. Sci. 49 (1) (1999) 581–632.
[3] P. Danielewicz, R. Lacey, W.G. Lynch, Determination of the equation of state of dense matter 298 (5598) (2002) 1592–1596.
[4] A. Andronic, J. Lukasik, W. Reisdorf, W. Trautmann, Systematics of stopping and flow in Au+Au collisions 30 (2006) 31–46.
[5] U. Heinz, R. Snellings, Collective flow and viscosity in relativistic heavy-ion collisions, Annu. Rev. Nucl. Part. Sci. 63 (2013) 123–151.
[6] S.-W. Lan, S.-S. Shi, Anisotropic flow in high baryon density region, Nucl. Sci. Tech. 33 (2) (2022) 21.
[7] M. Wang, J.-Q. Tao, H. Zheng, W.-C. Zhang, L.-L. Zhu, A. Bonasera, Number-of-constituent-quark scaling of elliptic flow: a quantitative study, Nucl. Sci. Tech. 33 (3) (2022) 37.
[8] C.-Z. Shi, Y.-G. Ma, α-clustering effect on flows of direct photons in heavy-ion collisions, Nucl. Sci. Tech. 32 (6) (2021) 66.
[9] Z.-W. Lin, L. Zheng, Further developments of a multi-phase transport model for relativistic nuclear collisions, Nucl. Sci. Tech. 32 (10) (2021) 113.
[10] M. Bleicher, E. Bratkovskaya, Modelling relativistic heavy-ion collisions with dynamical transport approaches, Prog. Part. Nucl. Phys. 122 (2022) 103920.
[11] B.-A. Li, L.-W. Chen, C.M. Ko, Recent progress and new challenges in isospin physics with heavy-ion reactions, Phys. Rep. 464 (4–6) (2008) 113–281.
[12] W. Reisdorf, Y. Leifels, A. Andronic, R. Averbeck, V. Barret, Z. Basrak, N. Bastid, M. Benabderrahmane, R. Čaplar, P. Crochet, et al., Systematics of azimuthal asymmetries in heavy ion collisions in the 1A GeV regime, Nucl. Phys. A 876 (2012) 1–60.
[13] M. Tsang, J. Stone, F. Camera, P. Danielewicz, S. Gandolfi, K. Hebeler, C.J. Horowitz, J. Lee, W.G. Lynch, Z. Kohley, et al., Constraints on the symmetry energy and neutron skins from experiments and theory, Phys. Rev. C 86 (1) (2012) 015803.
[14] P. Russotto, S. Gannon, S. Kupny, P. Lasko, L. Acosta, M. Adamczyk, A. Al-Ajlan, M. Al-Garawi, S. Al-Homaidhi, F. Amorini, et al., Results of the asy-eos experiment at GSI: the symmetry energy at suprasaturation density, Phys. Rev. C 94 (3) (2016) 034608.
[15] S. Huth, P.T. Pang, I. Tews, T. Dietrich, A. Le Fèvre, A. Schwenk, W. Trautmann, K. Agarwal, M. Bulla, M.W. Coughlin, et al., Constraining neutron-star matter with microscopic and macroscopic collisions, Nature 606 (7913) (2022) 276–280.
[16] H. Wolter, M. Colonna, D. Cozma, P. Danielewicz, C.M. Ko, R. Kumar, A. Ono, M.B. Tsang, J. Xu, Y.-X. Zhang, E. Bratkovskaya, Z.-Q. Feng, T. Gaitanos, A. Le Fèvre, N. Ikeno, Y. Kim, S. Mallik, P. Napolitani, D. Oliinychenko, T. Ogawa, M. Papa, J. Su, R. Wang, Y.-J. Wang, J. Weil, F.-S. Zhang, G.-Q. Zhang, Z. Zhang, J. Aichelin, W. Cassing, L.-W. Chen, H.-G. Cheng, H. Elfner, K. Gallmeister, C. Hartnack, S. Hashimoto, S. Jeon, K. Kim, M. Kim, B.-A. Li, C.-H. Lee, Q.-F. Li, Z.-X. Li, U. Mosel, Y. Nara, K. Niita, A. Ohnishi, T. Sato, T. Song, A. Sorensen, N. Wang, W.-J. Xie, TMEP collaboration, Transport model comparison studies of intermediate-energy heavy-ion collisions, Prog. Part. Nucl. Phys. 125 (2022) 103962.
[17] P. Li, Y. Wang, Q. Li, H. Zhang, Accessing the in-medium effects on nucleon-nucleon elastic cross section with collective flows and nuclear stopping, Phys. Lett. B 828 (2022) 137019.
[18] Y. Wang, C. Guo, Q. Li, A. Le Fèvre, Y. Leifels, W. Trautmann, Determination of the nuclear incompressibility from the rapidity-dependent elliptic flow in heavy-ion collisions at beam energies 0.4 A–1.0 A GeV, Phys. Lett. B 778 (2018) 207–212.
[19] J. Estee, W. Lynch, C. Tsang, J. Barney, G. Jhang, M. Tsang, R. Wang, M. Kaneko, J. Lee, T. Isobe, et al., Probing the symmetry energy with the spectral pion ratio, Phys. Rev. Lett. 126 (16) (2021) 162701.

[20] P. Morfouace, C. Tsang, Y. Zhang, W. Lynch, M. Tsang, D.D.S. Coupland, M. Youngs, Z. Chajecki, M. Famiano, T. Ghosh, et al., Constraining the symmetry energy with heavy-ion collisions and Bayesian analyses, Phys. Lett. B 799 (2019) 135045.
[21] J. Xu, Transport approaches for the description of intermediate-energy heavy-ion collisions, Prog. Part. Nucl. Phys. 106 (2019) 312–359.
[22] M. Colonna, Collision dynamics at medium and relativistic energies, Prog. Part. Nucl. Phys. 113 (2020) 103775.
[23] P. Danielewicz, R.A. Lacey, P.-B. Gossiaux, C. Pinkenburg, P. Chung, J. Alexander, R. McGrath, Disappearance of elliptic flow: a new probe for the nuclear equation of state, Phys. Rev. Lett. 81 (12) (1998) 2438.
[24] P. Danielewicz, Determination of the mean-field momentum-dependence using elliptic flow, Nucl. Phys. A 673 (1–4) (2000) 375–410.
[25] Y. Wang, Q. Li, Y. Leifels, A. Le Fèvre, Study of the nuclear symmetry energy from the rapidity-dependent elliptic flow in heavy-ion collisions around 1 GeV/nucleon regime, Phys. Lett. B 802 (2020) 135249.
[26] M. Cozma, Feasibility of constraining the curvature parameter of the symmetry energy using elliptic flow data, Eur. Phys. J. A 54 (3) (2018) 1–23.
[27] M. Abdallah, B. Aboona, J. Adam, L. Adamczyk, J. Adams, J. Adkins, G. Agakishiev, I. Aggarwal, M. Aggarwal, Z. Ahammed, et al., Light nuclei collectivity from $\sqrt{s_{NN}} = 3$ GeV Au+ Au collisions at RHIC, Phys. Lett. B 827 (2022) 136941.
[28] J. Adamczewski-Musch, O. Arnold, C. Behnke, A. Belounnas, et al., Directed, elliptic, and higher order flow harmonics of protons, deuterons, and tritons in Au + Au collisions at $\sqrt{s_{NN}} = 2.4$ GeV, Phys. Rev. Lett. 125 (2020) 262301.
[29] A. Le Fèvre, Y. Leifels, W. Reisdorf, J. Aichelin, C. Hartnack, Constraining the nuclear matter equation of state around twice saturation density, Nucl. Phys. A 945 (2016) 112–133.
[30] A. Le Fèvre, Y. Leifels, C. Hartnack, J. Aichelin, Origin of elliptic flow and its dependence on the equation of state in heavy ion reactions at intermediate energies, Phys. Rev. C 98 (3) (2018) 034901.
[31] Q. Li, C. Shen, C. Guo, Y. Wang, Z. Li, J. Lukasik, W. Trautmann, Nonequilibrium dynamics in heavy-ion collisions at low energies available at the GSI Schweri-onen Synchrotron, Phys. Rev. C 83 (2011) 044617.
[32] Y. Wang, C. Guo, Q. Li, H. Zhang, Z. Li, W. Trautmann, Collective flow of light particles in Au+ Au collisions at intermediate energies, Phys. Rev. C 89 (3) (2014) 034606.
[33] J. Xu, L.-W. Chen, M.B. Tsang, H. Wolter, Y.-X. Zhang, J. Aichelin, M. Colonna, D. Cozma, P. Danielewicz, Z.-Q. Feng, A. Le Fèvre, T. Gaitanos, C. Hartnack, K. Kim, Y. Kim, C.-M. Ko, B.-A. Li, Q.-F. Li, Z.-X. Li, P. Napolitani, A. Ono, M. Papa, T. Song, J. Su, J.-L. Tian, N. Wang, Y.-J. Wang, J. Weil, W.-J. Xie, F.-S. Zhang, G.-Q. Zhang, Understanding transport simulations of heavy-ion collisions at 100 and 400 A MeV: comparison of heavy-ion transport codes under controlled conditions, Phys. Rev. C 93 (2016) 044609.
[34] Y.-X. Zhang, N. Wang, Q.-F. Li, L. Ou, J.-L. Tian, M. Liu, K. Zhao, X.-Z. Wu, Z.-X. Li, Progress of quantum molecular dynamics model and its applications in heavy ion collisions, Front. Phys. 15 (5) (2020) 1–64.
[35] Y.-J. Wang, Q.-F. Li, Application of microscopic transport model in the study of nuclear equation of state from heavy ion collisions at intermediate energies, Front. Phys. 15 (4) (2020) 1–19.
[36] C. Hartnack, R.K. Puri, J. Aichelin, J. Konopka, S. Bass, H. Stoecker, W. Greiner, Modelling the many-body dynamics of heavy ion collisions: present status and future perspective, Eur. Phys. J. A 1 (2) (1998) 151–169.
[37] C. Hartnack, H. Oeschler, Y. Leifels, E.L. Bratkovskaya, J. Aichelin, Strangeness production close to the threshold in proton–nucleus and heavy-ion collisions, Phys. Rep. 510 (4–5) (2012) 119–200.
[38] Y. Zhang, Z. Li, C. Zhou, M.B. Tsang, Effect of isospin-dependent cluster recognition on the observables in heavy ion collisions, Phys. Rev. C 85 (2012) 051602.
[39] S.A. Bass, M. Belkacem, M. Bleicher, M. Brandstetter, L. Bravina, C. Ernst, L. Gerland, M. Hofmann, S. Hofmann, J. Konopka, et al., Microscopic models for ultrarelativistic heavy ion collisions, Prog. Part. Nucl. Phys. 41 (1998) 255–369.
[40] M. Bleicher, E. Zabrodin, C. Spieles, S.A. Bass, C. Ernst, S. Soff, L. Bravina, M. Belkacem, H. Weber, H. Stöcker, et al., Relativistic hadron-hadron collisions in the ultra-relativistic quantum molecular dynamics model, J. Phys. G, Nucl. Part. Phys. 25 (9) (1999) 1859.
[41] B. Zhang, M. Gyulassy, C.M. Ko, Elliptic flow from a parton cascade, Phys. Lett. B 455 (1–4) (1999) 45–48.
[42] J. Mohs, M. Ege, H. Elfner, M. Mayer, Collective flow at sis energies within a hadronic transport approach: influence of light nuclei formation and equation of state, Phys. Rev. C 105 (3) (2022) 034906.
[43] Z.-w. Lin, C.M. Ko, Partonic effects on the elliptic flow at relativistic heavy ion collisions, Phys. Rev. C 65 (3) (2002) 034904.
[44] W. Cassing, E. Bratkovskaya, Parton transport and hadronization from the dynamical quasiparticle point of view, Phys. Rev. C 78 (3) (2008) 034919.
[45] Z. Chen, Z. Wang, C. Greiner, Z. Xu, Splitting of elliptic flow in non-central relativistic heavy-ion collisions, arXiv preprint, arXiv:2108.12735, 2021.
[46] R. Marty, E. Bratkovskaya, W. Cassing, J. Aichelin, Observables in ultrarelativistic heavy-ion collisions from two different transport approaches for the same initial conditions, Phys. Rev. C 92 (1) (2015) 015201.
[47] L. Bravina, Y. Kvasiuk, S.Y. Sivoklokov, O. Vitiuk, E. Zabrodin, Anisotropic (v1 and v2) Flow in Relativistic Heavy-Ion Collisions at Energies Between 4 Gev and 200 Gev, EPJ Web of Conferences, vol. 191, EDP Sciences, 2018, p. 05004.
[48] L. Shi, P. Danielewicz, R. Lacey, Spectator response to the participant blast, Phys. Rev. C 64 (3) (2001) 034601.
[49] R.S. Bhalerao, J.-P. Blaizot, N. Borghini, J.-Y. Ollitrault, Elliptic flow and incomplete equilibration at rhic, Phys. Lett. B 627 (1–4) (2005) 49–54.
[50] C. Gombeaud, J.-Y. Ollitrault, Covariant transport theory approach to elliptic flow in relativistic heavy ion collision, Phys. Rev. C 77 (5) (2008) 054904.
[51] S. Vogel, G. Torrieri, M. Bleicher, Elliptic flow fluctuations in heavy ion collisions and the perfect fluid hypothesis, Phys. Rev. C 82 (2) (2010) 024908.
[52] Y. Liu, Y. Wang, Y. Cui, C.-J. Xia, Z. Li, Y. Chen, Q. Li, Y. Zhang, Insights into the pion production mechanism and the symmetry energy at high density, Phys. Rev. C 103 (1) (2021) 014616.